A Fourier Pseudospectral Method for the “Good” Boussinesq Equation with Second-Order Temporal Accuracy

Kelong Cheng,[1] **Wenqiang Feng,**[2] **Sigal Gottlieb,**[3] **Cheng Wang**[3]

[1] *Department of Mathematics, Southwest University of Science and Technology, Mianyang, Sichuan 621010, People's Republic of China*

[2] *Department of Mathematics, University of Tennessee, Knoxville, Tennessee 37996*

[3] *Department of Mathematics, University of Massachusetts, North Dartmouth, Massachusetts 02747*

Received 24 January 2014; accepted 22 May 2014
Published online 24 June 2014 in Wiley Online Library (wileyonlinelibrary.com).
DOI 10.1002/num.21899

In this article, we discuss the nonlinear stability and convergence of a fully discrete Fourier pseudospectral method coupled with a specially designed second-order time-stepping for the numerical solution of the “good” Boussinesq equation. Our analysis improves the existing results presented in earlier literature in two ways. First, a $\ell^\infty(0, T^*; H^2)$ convergence for the solution and $\ell^\infty(0, T^*; \ell^2)$ convergence for the time-derivative of the solution are obtained in this article, instead of the $\ell^\infty(0, T^*; \ell^2)$ convergence for the solution and the $\ell^\infty(0, T^*; H^{-2})$ convergence for the time-derivative, given in De Frutos, et al., Math Comput 57 (1991), 109–122. In addition, we prove that this method is unconditionally stable and convergent for the time step in terms of the spatial grid size, compared with a severe restriction time step restriction $\Delta t \le Ch^2$ required by the proof in De Frutos, et al., Math Comput 57 (1991), 109–122.
Numer Methods Partial Differential Eq 31: 202–224, 2015

Keywords: aliasing error; fully discrete Fourier pseudospectral method; good Boussinesq equation; stability and convergence

I. INTRODUCTION

The soliton-producing nonlinear wave equation is a topic of significant scientific interest. One commonly used example is the so-called “good” Boussinesq (GB) equation

$$u_{tt} = -u_{xxxx} + u_{xx} + (u^p)_{xx}, \quad \text{with an integer } p \ge 2. \tag{1.1}$$

Correspondence to: Cheng Wang, Department of Mathematics, University of Massachusetts, 285 Old Westport Road, North Dartmouth, MA 02747 (e-mail: cwang1@umassd.edu)
Contract grant sponsor: Air Force Office of Scientific Research (to S. G); contract grant number: FA-9550-12-1-0224
Contract grant sponsor: NSF (to C. W); contract grant number: DMS-1115420
Contract grant sponsor: NSFC (to C. W.); contract grant number: 11271281

It is similar to the well-known Korteweg-de Vries (KdV) equation; a balance between dispersion and nonlinearity leads to the existence of solitons. The GB equation and its various extensions have been investigated by many authors. For instance, a closed form solution for the two soliton interaction of Eq. (1.1) was obtained by Manoranjan et al. in [1] and a few numerical experiments were performed based on the Petrov–Galerkin method with linear "hat" functions. In [2], it was shown that the GB equation possesses a highly complicated mechanism for the solitary waves interaction. Ortega and Sanz-Serna [3] discussed nonlinear stability and convergence of some simple finite difference schemes for the numerical solution of this equation. More analytical and numerical works related to GB equations can be found in the literature, for example, [4–15].

In this article, we consider the GB equation (1.1), with a periodic boundary condition over an one-dimensional (1D) domain $\Omega = (0,L)$ and initial data $u(x,0) = u^0(x), u_t(x,0) = v^0(x)$, both of which are L-periodic. It is assumed that a unique, periodic, smooth enough solution exists for (1.1) over the time interval $(0,T)$. This L-periodicity assumption is reasonable if the solution to (1.1) decays exponentially outside $[0,L]$.

Due to the periodic boundary condition, the Fourier collocation (pseudospectral) differentiation is a natural choice to obtain the optimal spatial accuracy. There has been a wide and varied literature on the development of spectral and pseudospectral schemes. For instance, the stability analysis for linear time-dependent problems can be found in [16, 17], and so forth, based on eigenvalue estimates. Some pioneering works for nonlinear equations were initiated by Maday and Quarteroni [18–20] for steady-state spectral solutions. Also, note the analysis of 1D conservation laws by Tadmor and coworkers [21–27], semidiscrete viscous Burgers' equation and Navier–Stokes equations by Weinan [28, 29], the Galerkin spectral method for Navier–Stokes equations led by Guo [22, 30–32] and Shen [33, 34], and the fully discrete (discrete both in space and time) pseudospectral method applied to viscous Burgers' equation in [11] by Gottlieb and Wang and [35] by Bressan and Quarteroni, and so forth.

In addition, an application of spectral and pseudospectral approximation to dispersive nonlinear wave equation, such as KdV equation has attracted a great deal of attention. Many interesting theoretical analysis and numerical results have been reported in the existing literature; for example, see [36] for the semidiscrete spectral methods, [37] for the error estimate of a fully discrete scheme, and [38, 39] for the error estimates of the Benjamin–Ono equation or related nonlocal models, and so forth. For the GB equation (1.1), it is worth mentioning De Frutos et al.'s work [10] on the nonlinear analysis of a second-order (in time) pseudospectral scheme for the GB equation (with $p = 2$). However, as the authors point out in their remark on page 119, these theoretical results were not optimal: "... our energy norm is an L^2-norm of u combined with a negative norm of u_t. This should be compared with the energy norm in [40]: there, no integration with respect to x is necessary and convergence is proved in H^2 for u and L^2 for u_t." The difficulties in the analysis are due to the absence of a dissipation mechanism in the GB equation (1.1), which makes the nonlinear error terms much more challenging to analyze than that of a parabolic equation. The presence of a second-order spatial derivative for the nonlinear term leads to an essential difficulty of numerical error estimate in a higher order Sobolev norm. In addition to the lack of optimal numerical error estimate, the analysis in [10] also imposes a severe time step restriction: $\Delta t \le Ch^2$ (with C a fixed constant), in the nonlinear stability analysis. Such a constraint becomes very restrictive for a fine numerical mesh and leads to a high computational cost.

In this work, we propose a second-order (in time) pseudospectral scheme for the GB equation (1.1) with an alternate approach, and provide a novel nonlinear analysis. In more detail, a $\ell^\infty(0,T^*;H^2)$ convergence for u and $\ell^\infty(0,T^*;\ell^2)$ convergence for u_t are derived, compared with the $\ell^\infty(0,T^*;\ell^2)$ convergence for u and $\ell^\infty(0,T^*;H^{-2})$ convergence for u_t, as reported in [10].

Furthermore, such a convergence is unconditional (for the time step Δt in terms of space grid size h) so that the severe time step constraint $\Delta t \leq Ch^2$ is avoided.

The methodology of the proposed second-order temporal discretization is very different from that in [10]. To overcome the difficulty associated with the second-order temporal derivative in the hyperbolic equation, we introduce a new variable ψ to approximate u_t, which greatly facilitates the numerical implementation. Conversely, the corresponding second-order consistency analysis becomes nontrivial because of a $O(\Delta t^2)$ numerical error between the centered difference of u and the midpoint average of ψ. Without a careful treatment, such a $O(\Delta t^2)$ numerical error might seem to introduce a reduction of temporal accuracy, because of the second-order time derivative involved in the equation. To overcome this difficulty, we perform a higher order consistency analysis by an asymptotic expansion; as a result, the constructed approximate solution satisfies the numerical scheme with a higher order truncation error. Furthermore, a projection of the exact solution onto the Fourier space leads to an optimal regularity requirement.

For the nonlinear stability and convergence analysis, we have to obtain a direct estimate of the (discrete) H^2 norm of the nonlinear numerical error function. This estimate relies on the aliasing error control lemma for pseudospectral approximation to nonlinear terms, which was proven in a recent work [11]. That is the key reason we are able to overcome the key difficulty in the nonlinear estimate and obtain a $\ell^\infty(0, T^*; H^2)$ convergence for u and $\ell^\infty(0, T^*; \ell^2)$ convergence for u_t. We prove that the proposed numerical scheme is fully consistent (with a higher order expansion), stable and convergent in the H^2 norm up to some fixed final time T^*. In turn, the maximum norm bound of the numerical solution is automatically obtained, because of the H^2 error estimate and the corresponding Sobolev embedding. Therefore, the inverse inequality in the stability analysis is not needed and any scaling law between Δt and h is avoided, compared with the $\Delta t \leq Ch^2$ constraint reported in [10].

This article is outlined as follows. In Section II, we review the Fourier spectral and pseudospectral differentiation, recall an aliasing error control lemma (proven in [11]), and present an alternate second-order (in time) pseudospectral scheme for the GB equation (1.1). In Section III, the consistency analysis of the scheme is studied in detail. The stability and convergence analysis is reported in Section IV. A simple numerical result is presented in Section V. Finally, some concluding remarks are made in Section VI.

II. THE NUMERICAL SCHEME AND THE MAIN RESULT

A. Review of Fourier Spectral and Pseudospectral Approximations

For $f(x) \in L^2(\Omega), \Omega = (0, L)$, with Fourier series

$$f(x) = \sum_{l=-\infty}^{\infty} \hat{f}_l e^{2\pi i l x/L}, \quad \text{with} \quad \hat{f}_l = \int_\Omega f(x) e^{-2\pi i l x/L} dx, \tag{2.1}$$

its truncated series is defined as the projection onto the space $\mathcal{B}^N$ of trigonometric polynomials in x of degree up to N, given by

$$\mathcal{P}_N f(x) = \sum_{l=-N}^{N} \hat{f}_l e^{2\pi i l x/L}. \tag{2.2}$$

To obtain a pseudospectral approximation at a given set of points, an interpolation operator $\mathcal{I}_N$ is introduced. Given a uniform numerical grid with $(2N+1)$ points and a discrete vector function $\mathbf{f}$ where $\mathbf{f}_i = f(x_i)$, for each spatial point x_i. The Fourier interpolation of the function is defined by

$$(\mathcal{I}_N f)(x) = \sum_{l=-N}^{N} (\hat{f}_c^N)_l e^{2\pi i l x/L}, \tag{2.3}$$

where the $(2N+1)$ pseudospectral coefficients $(\hat{f}_c^N)_l$ are computed based on the interpolation condition $f(x_i) = (\mathcal{I}_N f)(x_i)$ on the $2N+1$ equidistant points [41–43]. These collocation coefficients can be efficiently computed using the fast Fourier transform (FFT). Note that the pseudospectral coefficients are not equal to the actual Fourier coefficients; the difference between them is known as the aliasing error. In general, $\mathcal{P}_N f(x) \neq \mathcal{I}_N f(x)$, and even $\mathcal{P}_N f(x_i) \neq \mathcal{I}_N f(x_i)$, except of course in the case that $f \in \mathcal{B}^N$.

The Fourier series and the formulas for its projection and interpolation allow one to easily take derivative by simply multiplying the appropriate Fourier coefficients $(\hat{f}_c^N)_l$ by $2l\pi i/L$. Furthermore, we can take subsequent derivatives in the same way, so that differentiation in physical space is accomplished via multiplication in Fourier space. As long as f and all is derivatives (up to mth order) are continuous and periodic on Ω, the convergence of the derivatives of the projection and interpolation is given by

$$\begin{aligned} ||\partial^k f(x) - \partial^k \mathcal{P}_N f(x)|| &\leq C||f^{(m)}||h^{m-k}, \quad \text{for } 0 \leq k \leq m, \\ ||\partial^k f(x) - \partial^k \mathcal{I}_N f(x)|| &\leq C||f||_{H^m} h^{m-k}, \quad \text{for } 0 \leq k \leq m,\ m > \frac{d}{2}, \end{aligned} \tag{2.4}$$

in which $\|\cdot\|$ denotes the L^2 norm. For more details, see the discussion of approximation theory by Canuto and Quarteroni [44].

For any collocation approximation to the function $f(x)$ at the points x_i

$$f(x_i) = (\mathcal{I}_N f)_i = \sum_{l=-N}^{N} (\hat{f}_c^N)_l e^{2\pi i l x_i}, \tag{2.5}$$

one can define discrete differentiation operator $\mathcal{D}_N$ operating on the vector of grid values $\mathbf{f} = f(x_i)$. In practice, one may compute the collocation coefficients $(\hat{f}_c^N)_l$ via FFT, and then multiply them by the correct values (given by $2l\pi i$) and perform the inverse FFT. Alternatively, we can view the differentiation operator $\mathcal{D}_N$ as a matrix, and the above process can be seen as a matrix-vector multiplication. The same process is performed for the second and fourth derivatives ∂_x^2, ∂_x^4, where this time the collocation coefficients are multiplied by $(-4\pi^2 l^2/L^2)$ and $(16\pi^4 l^4/L^4)$, respectively. In turn, the differentiation matrix can be applied for multiple times, that is, the vector $\mathbf{f}$ is multiplied by $\mathcal{D}_N^2$ and $\mathcal{D}_N^4$, respectively.

Because the pseudospectral differentiation is taken at a point-wise level, a discrete L^2 norm and inner product need to be introduced to facilitate the analysis. Given any periodic grid functions $\mathbf{f}$ and $\mathbf{g}$ (over the numerical grid), we note that these are simply vectors and define the discrete L^2 inner product and norm

$$\|\mathbf{f}\|_2 = \sqrt{\langle \mathbf{f}, \mathbf{f} \rangle}, \quad \text{with} \quad \langle \mathbf{f}, \mathbf{g} \rangle = \frac{1}{2N+1} \sum_{i=0}^{2N} \mathbf{f}_i \mathbf{g}_i. \tag{2.6}$$

The following summation by parts (see [11]) will be of use:

$$\langle \mathbf{f}, \mathcal{D}_N \mathbf{g} \rangle = -\langle \mathcal{D}_N \mathbf{f}, \mathbf{g} \rangle, \quad \langle \mathbf{f}, \mathcal{D}_N^2 \mathbf{g} \rangle = -\langle \mathcal{D}_N \mathbf{f}, \mathcal{D}_N \mathbf{g} \rangle, \quad \langle \mathbf{f}, \mathcal{D}_N^4 \mathbf{g} \rangle = \langle \mathcal{D}_N^2 \mathbf{f}, \mathcal{D}_N^2 \mathbf{g} \rangle. \tag{2.7}$$

B. An Aliasing Error Control Estimate in Fourier Pseudospectral Approximation

This lemma, established in [11], allows us to bound the aliasing error for the nonlinear term, and will be critical to our analysis. For any function $\varphi(x)$ in the space $\mathcal{B}^{pN}$, its collocation coefficients $\hat{q}_l^N$ are computed based on the $2N + 1$ equidistant points. In turn, $\mathcal{I}_N \varphi(x)$ is given by the continuous expansion based on these coefficients:

$$\mathcal{I}_N \varphi(x) = \sum_{l=-N}^{N} \hat{q}_l^N \mathrm{e}^{2\pi \mathrm{i} l x/L}. \tag{2.8}$$

Since $\varphi(x) \in \mathcal{B}^{pN}$, we have $\mathcal{I}_N \varphi(x) \neq \mathcal{P}_N \varphi(x)$ due to the aliasing error.

The following lemma enables us to obtain an H^m bound of the interpolation of the nonlinear term; the detailed proof can be found in [11].

Lemma 2.1. *For any $\varphi \in \mathcal{B}^{pN}$ (with p an integer) in dimension d, we have*

$$\|\mathcal{I}_N \varphi\|_{H^k} \leq (\sqrt{p})^d \|\varphi\|_{H^k}. \tag{2.9}$$

C. Formulation of the Numerical Scheme and the Convergence Result

We propose the following fully discrete second-order (in time) scheme for Eq. (1.1):

$$\begin{cases} \dfrac{\psi^{n+1} - \psi^n}{\Delta t} = - D_N^4 \left(\dfrac{u^{n+1} + u^n}{2} \right) + D_N^2 \left(\dfrac{u^{n+1} + u^n}{2} \right) + D_N^2 \left(\dfrac{3}{2}(u^n)^p - \dfrac{1}{2}(u^{n-1})^p \right), \\ \dfrac{u^{n+1} - u^n}{\Delta t} = \dfrac{\psi^{n+1} + \psi^n}{2}, \end{cases} \tag{2.10}$$

where ψ is a second-order approximation to u_t and D_N denotes the discrete differentiation operator.

The main result of this article is given later.

Theorem 2.2. *For any final time $T > 0$, assume the exact solution u_e to the GB equation (1.1) given by (3.21). Denote $u_{\Delta t,h}$ as the continuous (in space) extension of the fully discrete numerical solution given by scheme (2.10). As $\Delta t, h \to 0$, the following convergence result is valid:*

$$\|u_{\Delta t,h} - u_e\|_{\ell^\infty(0,T^*;H^2)} + \|\psi_{\Delta t,h} - \psi_e\|_{\ell^\infty(0,T^*;L^2)} \leq C(\Delta t^2 + h^m), \tag{2.11}$$

provided that the time step Δt and the space grid size h are bounded by given constants which are only dependent on the exact solution. Note that the convergence constant in (2.11) also depends on the exact solution as well as T.

Remark 2.3. With a substitution $\psi^{n+1} = \frac{2(u^{n+1}-u^n)}{\Delta t} - \psi^n$, the scheme (2.10) can be reformulated as a closed equation for u^{n+1}:

$$\frac{2u^{n+1}}{\Delta t^2} + \frac{1}{2}(D_N^4 - D_N^2)u^{n+1} = D_N^2 \left(\frac{3}{2}(u^n)^p - \frac{1}{2}(u^{n-1})^p \right) - \frac{1}{2}(D_N^4 - D_N^2)u^n + \frac{\frac{2u^n}{\Delta t} + 2\psi^n}{\Delta t}. \tag{2.12}$$

As the treatment of the nonlinear term is fully explicit, this resulting implicit scheme requires only a linear solver. Furthermore, a detailed calculation shows that all the eigenvalues of the linear operator on the left-hand side are positive, and so the unique unconditional solvability of the proposed scheme (2.10) is assured. In practice, the FFT can be used to efficiently obtain the numerical solutions.

Remark 2.4. An introduction of the variable ψ allows us to rewrite the wave equation as a first-order system in time. This rewritten form not only facilitates the numerical implementation, but also improves the numerical stability. The stability analysis and error estimate for the linear version of (2.10) were provided in an earlier article [45].

Remark 2.5. In contrast, three time steps t^{n+1}, t^n, and t^{n-1} are involved in the numerical approximation to the second-order temporal derivative as presented in the earlier work [10] (with $p = 2$):

$$\frac{u^{n+1} - 2u^n + u^{n-1}}{\Delta t^2} = -\frac{1}{4} D_N^4 (u^{n+1} + 2u^n + u^{n-1}) + D_N^2 u^n + D_N^2((u^n)^2). \tag{2.13}$$

A careful analysis in [10] shows that the numerical stability for (2.13) could only be theoretically justified under a severe time step constraint $\Delta t \le Ch^2$, although an intuitive and linearized stability analysis, as well as the numerical results, indicate that a standard Courant–Friedrichs–Lewy (CFL) condition $\Delta t = O(h)$ is sufficient. Conversely, the special structure of our proposed scheme (2.10) results in an unconditional stability and convergence for a fixed final time, as will be presented in later analysis.

These subtle differences in terms of the stability conditions will be analyzed in later sections. See Remarks 4.3–4.6 below.

III. THE CONSISTENCY ANALYSIS

In this section, we establish a truncation error estimate for the fully discrete scheme (2.10) for the GB equation (1.1). A finite Fourier projection is applied to the exact solution of the GB equation (1.1) and a local truncation error is derived. Moreover, we perform a higher order consistency analysis in time, through an addition of a correction term, so that the constructed approximate solution satisfies the numerical scheme with higher order temporal accuracy. This approach avoids a key difficulty associated with the accuracy reduction in time due to the appearance of the second in time temporal derivative.

A. Truncation Error Analysis for U_N

Given the domain $\Omega = (0,L)$, the uniform mesh grid (x_i), $0 \le i \le 2N$, and the exact solution u_e, we denote U_N as its projection into $\mathcal{B}^N$:

$$U_N(x,t) := \mathcal{P}_N u_e(x,t). \tag{3.1}$$

The following approximation estimates are clear:

$$\|U_N - u_e\|_{L^\infty(0,T^*;H^r)} \le Ch^m \|u_e\|_{L^\infty(0,T^*;H^{m+r})}, \quad \text{for } r \ge 0, \tag{3.2}$$

$$\|\partial_t^k (U_N - u_e)\|_{H^r} \le Ch^m \|\partial_t^k u_e\|_{H^{m+r}}, \quad \text{for } r \ge 0,\ 0 \le k \le 4, \tag{3.3}$$

in which the second inequality comes from the fact that $\partial_t^k U_N$ is the truncation of $\partial_t^k u_e$ for any $k \geq 0$, as projection and differentiation commute:

$$\frac{\partial^k}{\partial t^k} U_N(\mathbf{x}, t) = \frac{\partial^k}{\partial t^k} \mathcal{P}_N u_e(x, t) = \mathcal{P}_N \frac{\partial^k u_e(x, t)}{\partial t^k}. \tag{3.4}$$

As a direct consequence, the following linear estimates are straightforward:

$$\|\partial_t^2 (U_N - u_e)\|_{L^2} \leq C h^m \|\partial_t^2 u_e\|_{H^m}, \tag{3.5}$$

$$\|\partial_x^2 (U_N - u_e)\|_{L^2} \leq C h^m \|u_e\|_{H^{m+2}}, \quad \|\partial_x^4 (U_N - u_e)\|_{L^2} \leq C h^m \|u_e\|_{H^{m+4}}. \tag{3.6}$$

Conversely, a discrete $\|\cdot\|_2$ estimate for these terms is needed in the local truncation derivation. To overcome this difficulty, we observe that

$$\|\partial_t^2 (U_N - u_e)\|_2 = \|\mathcal{I}_N (\partial_t^2 (U_N - u_e))\|_{L^2} \leq \|\partial_t^2 (U_N - u_e)\|_{L^2} + \|\partial_t^2 (\mathcal{I}_N u_e - u_e)\|_{L^2}, \tag{3.7}$$

in which the second step comes from the fact that $\mathcal{I}_N \partial_t^2 U_N = \partial_t^2 U_N$, since $\partial_t^2 U_N \in \mathcal{B}^N$. The first term has an estimate given by (3.5), whereas the second term could be bounded by

$$\|(\partial_t^2 (\mathcal{I}_N u_e - u_e))\|_{L^2} = \|\mathcal{I}_N (\partial_t^2 u_e) - \partial_t^2 u_e\|_{L^2} \leq C h^m \|\partial_t^2 u_e\|_{H^m}, \tag{3.8}$$

as an application of (2.4). In turn, its combination with (3.7) and (3.5) yields

$$\|\partial_t^2 (U_N - u_e)\|_2 \leq C h^m \|\partial_t^2 u_e\|_{H^m}. \tag{3.9}$$

Using similar arguments, we also arrive at

$$\|\partial_x^2 (U_N - u_e)\|_2 \leq C h^m \|u_e\|_{H^{m+2}}, \quad \|\partial_x^4 (U_N - u_e)\|_2 \leq C h^m \|u_e\|_{H^{m+4}}. \tag{3.10}$$

For the nonlinear term, we begin with the following expansion:

$$\partial_x^2 (u_e^p) = p((p-1) u_e^{p-2} (u_e)_x^2 + u_e^{p-1} (u_e)_{xx}), \quad \text{which in turn gives}$$

$$\begin{aligned} \partial_x^2 (u_e^p - (U_N)^p) = p\Bigg(& (p-1) U_N^{p-2} (u_e + U_N)_x (u_e - U_N)_x \\ & + (p-1)(u_e - U_N)(u_e)_x^2 \sum_{k=0}^{p-3} u_e^k U_N^{p-3-k} \\ & + U_N^{p-1} (u_e - U_N)_{xx} + (u_e - U_N)(u_e)_{xx} \sum_{k=0}^{p-2} u_e^k U_N^{p-2-k} \Bigg). \end{aligned} \tag{3.11}$$

Subsequently, its combination with (3.2) implies that

$$\begin{aligned} & \|\partial_x^2 (u_e^p - (U_N)^p)\|_{L^2} \\ & \leq C(\|U_N\|_{L^\infty}^{p-2} \cdot \|u_e + U_N\|_{W^{1,\infty}} \cdot \|u_e - U_N\|_{H^1} + \|U_N\|_{L^\infty}^{p-1} \cdot \|u_e - U_N\|_{H^2} \\ & \quad + \|u_e - U_N\|_{L^\infty} \cdot (\|u_e\|_{L^\infty}^{p-2} + \|U_N\|_{L^\infty}^{p-2}) \cdot (\|u_e\|_{H^2} + \|u_e\|_{W^{1,4}}^2)) \\ & \leq C(\|U_N\|_{H^1}^{p-2} \cdot \|u_e + U_N\|_{H^2} \cdot \|u_e - U_N\|_{H^1} + \|U_N\|_{H^1}^{p-1} \cdot \|u_e - U_N\|_{H^2} \\ & \quad + \|u_e - U_N\|_{H^1} \cdot (\|u_e\|_{H^1}^{p-2} + \|U_N\|_{H^1}^{p-2}) \cdot (\|u_e\|_{H^2} + \|u_e\|_{H^2}^2)) \end{aligned}$$

$$\leq C(\|u_e\|_{H^2}^p + \|U_N\|_{H^2}^p) \cdot \|u_e - U_N\|_{H^2}$$
$$\leq C\|u_e\|_{H^2}^p \cdot \|u_e - U_N\|_{H^2} \leq Ch^m \|u_e\|_{H^2}^p \cdot \|u_e\|_{H^{m+2}}, \tag{3.12}$$

in which an 1D Sobolev embedding was used in the second step.

The following interpolation error estimates can be derived in a similar way, based on (2.4):

$$\|\partial_x^2(u_e^p) - \mathcal{I}_N(\partial_x^2(u_e^p))\|_{L^2} \leq Ch^m \|\partial_x^2(u_e^p)\|_{H^m} \leq Ch^m \|u_e\|_{H^2}^p \cdot \|u_e\|_{H^{m+2}}, \tag{3.13}$$
$$\|\partial_x^2(U_N^p) - \mathcal{I}_N(\partial_x^2(U_N^p))\|_{L^2} \leq Ch^m \|\partial_x^2(U_N^p)\|_{H^m} \leq Ch^m \|u_e\|_{H^2}^p \cdot \|u_e\|_{H^{m+2}}. \tag{3.14}$$

In turn, a combination of (3.12)–(3.14) implies the following estimate for the nonlinear term

$$\begin{aligned}\|\partial_x^2(u_e^p - (U_N)^p)\|_2 &= \|\mathcal{I}_N(\partial_x^2(u_e^p - (U_N)^p))\|_{L^2} \\ &\leq \|\partial_x^2(u_e^p - (U_N)^p)\|_{L^2} + \|\partial_x^2(u_e^p) - \mathcal{I}_N(\partial_x^2(u_e^p))\|_{L^2} \\ &\quad + \|\partial_x^2(U_N^p) - \mathcal{I}_N(\partial_x^2(U_N^p))\|_{L^2} \leq Ch^m \|u_e\|_{H^2}^p \cdot \|u_e\|_{H^{m+2}}.\end{aligned} \tag{3.15}$$

By observing (3.9), (3.10), and (3.15), we conclude that U_N satisfies the original GB equation (1.1) up to a $O(h^m)$ (spectrally accurate) truncation error:

$$\partial_t^2 U_N = -\partial_x^4 U_N + \partial_x^2 U_N + \partial_x^2(U_N^p) + \tau_0, \quad \text{with } \|\tau_0\|_2 \leq Ch^m(\|u_e\|_{H^2}^p + 1) \cdot \|u_e\|_{H^{m+4}}. \tag{3.16}$$

Moreover, we define the following profile, a second-order (in time) approximation to $\partial_t u_e$:

$$\Psi_N(x,t) := \partial_t U_N(x,t) - \frac{\Delta t^2}{12}\partial_t^3 U_N(x,t). \tag{3.17}$$

For any function $G = G(x,t)$, given $n > 0$, we define $G^n(x) := G(x, n\Delta t)$.

B. Truncation Error Analysis in Time

For simplicity of presentation, we assume $T = K\Delta t$ with an integer K. The following two preliminary estimates are excerpted from a recent work [46], which will be useful in later consistency analysis.

Proposition 3.1 ([46]). *For $f \in H^3(0,T)$, we have*

$$\|\tau^t f\|_{\ell^2(0,T)} \leq C\Delta t^m \|f\|_{H^{m+1}(0,T)}, \quad \textit{with} \quad \tau^t f^n = \frac{f^{n+1} - f^n}{\Delta t} - f'(t^{n+1/2}), \tag{3.18}$$

for $0 \leq m \leq 2$, where C only depends on T, $\|\cdot\|_{\ell^2(0,T)}$ is a discrete L^2 norm (in time) given by $\|g\|_{\ell^2(0,T)} = \sqrt{\Delta t \sum_{n=0}^{K-1}(g^n)^2}$.

Proposition 3.2 ([46]). *For $f \in H^2(0,T)$, we have*

$$\|D_{t/2}^2 f\|_{\ell^2(0,T)} := \left(\Delta t \sum_{n=0}^{K-1}\left(D_{t/2}^2 f^{n+1/2}\right)^2\right)^{\frac{1}{2}} \leq C\|f\|_{H^2(0,T)}, \tag{3.19}$$

$$\|D_t^2 f\|_{\ell^2(0,T)} := \left(\Delta t \sum_{n=0}^{K-1} \left(D_t^2 f^n\right)^2\right)^{\frac{1}{2}} \le C\|f\|_{H^2(0,T)},$$

$$\text{with} \quad D_{t/2}^2 f^{n+1/2} = \frac{4(f^{n+1} - 2f(\,\cdot\,, t^{n+1/2}) + f^n)}{\Delta t^2}, \quad D_t^2 f^n = \frac{f^{n+1} - 2f^n + f^{n-1}}{\Delta t^2}, \tag{3.20}$$

where C only depends on T.

The following theorem is the desired consistency result. To simplify the presentation below, for the constructed solution (U_N, ψ_N), we define its vector grid function $(U^n, \Psi^n) = \mathcal{I}(U_N, \psi_N)$ as its interpolation: $U_i^n = U_N^n(x_i, t^n)$, $\Psi_i^n = \Psi_N^n(x_i, t^n)$.

Theorem 3.1. *Suppose the unique periodic solution for Eq. (1.1) satisfies the following regularity assumption*

$$u_\mathrm{e} \in H^4(0,T;L^2) \cap L^\infty(0,T;H^{m+4}) \cap H^2(0,T;H^4). \tag{3.21}$$

Set (U_N, Ψ_N) as the approximation solution constructed by (3.1), (3.17) and let (U, Ψ) as its discrete interpolation. Then, we have

$$\begin{cases} \dfrac{\Psi^{n+1} - \Psi^n}{\Delta t} = -D_N^4\left(\dfrac{U^{n+1} + U^n}{2}\right) + D_N^2\left(\dfrac{U^{n+1} + U^n}{2}\right) + D_N^2\left(\dfrac{3}{2}(U^n)^p - \dfrac{1}{2}(U^{n-1})^p\right) + \tau_1^n, \\ \dfrac{U^{n+1} - U^n}{\Delta t} = \dfrac{\Psi^{n+1} + \Psi^n}{2} + \Delta t \tau_2^n, \end{cases} \tag{3.22}$$

where τ_i^k satisfies

$$\|\tau_i\|_{\ell^2(0,T;\ell^2)} := \left(\Delta t \sum_{k=0}^{K} \|\tau_i^k\|_2^2\right)^{\frac{1}{2}} \le M(\Delta t^2 + h^m), \quad i = 1, 2, \tag{3.23}$$

in which M only depends on the regularity of the exact solution u_e.

Proof. We define the following notation:

$$\begin{aligned} F_0^{n+1/2} &= \tfrac{U^{n+1} - U^n}{\Delta t}, & & \\ F_1^{n+1/2} &= \tfrac{\Psi^{n+1} - \Psi^n}{\Delta t}, & F_{1e}^{n+1/2} &= (\partial_t^2 U_N)(\cdot, t^{n+1/2}), \\ F_2^{n+1/2} &= D_N^4 U^{n+1/2}, & F_{2e}^{n+1/2} &= (\partial_x^4 U_N)(\cdot, t^{n+1/2}), \\ F_3^{n+1/2} &= D_N^2 U^{n+1/2}, & F_{2e}^{n+1/2} &= (\partial_x^2 U_N)(\cdot, t^{n+1/2}), \\ F_4^{n+1/2} &= D_N^2(\tfrac{3}{2}(U^p)^n - \tfrac{1}{2}(U^p)^{n-1}), & F_{4e}^{n+1/2} &= (\partial_x^2 U_N^2)(\cdot, t^{n+1/2}), \\ F_5^{n+1/2} &= \tfrac{\Psi^{n+1} + \Psi^n}{2}. & & \end{aligned} \tag{3.24}$$

Note that the quantities on the left side are defined on the numerical grid (in space) point-wise, whereas the ones on the right-hand side are continuous functions.

To begin with, we look at the second-order time derivative terms, F_1 and F_{1e}. From the definition (3.17), we get

$$F_1^{n+1/2} = \frac{\partial_t u_N^{n+1} - \partial_t u_N^n}{\Delta t} - \frac{\Delta t^2}{12}\frac{\partial_t^3 u_N^{n+1} - \partial_t^3 u_N^n}{\Delta t} := F_{11}^{n+1/2} - \frac{\Delta t^2}{12} F_{12}^{n+1/2}, \tag{3.25}$$

at a point-wise level, where F_{11} and F_{12} are the finite difference (in time) approximation to $\partial_t^2 U_N$, $\partial_t^4 U_N$, respectively. We define F_{11e} and F_{12e} in a similar way as (3.24), that is,

$$F_{11e}^{n+1/2} = \partial_t^2 U_N(\cdot, t^{n+1/2}), \quad F_{12e}^{n+1/2} = \partial_t^4 U_N(\cdot, t^{n+1/2}). \tag{3.26}$$

The following estimates can be derived by using Proposition 3.1 (with $m = 2$ and $m = 0$):

$$\|F_{11} - F_{11e}\|_{\ell^2(0,T)} \le C\Delta t^2 \|U_N\|_{H^4(0,T)}, \quad \|F_{12} - F_{12e}\|_{\ell^2(0,T)} \le C\|U_N\|_{H^4(0,T)}, \tag{3.27}$$

for each fixed grid point. This in turn yields

$$\|F_1 - F_{1e}\|_{\ell^2(0,T)} \le C\Delta t^2 \|U_N\|_{H^4(0,T)}. \tag{3.28}$$

In turn, an application of discrete summation in Ω leads to

$$\|F_1 - \mathcal{I}(F_{1e})\|_{\ell^2(0,T;\ell^2)} \le C\Delta t^2 \|U_N\|_{H^4(0,T;L^2)} \le C\Delta t^2 \|u_e\|_{H^4(0,T;L^2)}, \tag{3.29}$$

due to the fact that $U_N \in \mathcal{B}^N$, and (3.3) was used in the second step.

For the terms F_2 and F_{2e}, we start from the following observation (recall that $U_N^{k+1/2} = \frac{U_N^{k+1} + U_N^k}{2}$)

$$\|F_2^{n+1/2} - \mathcal{I}(\partial_x^4 U_N^{n+1/2})\|_2 \equiv 0, \quad \text{since } U_N^{n+1/2} \in \mathcal{B}^N. \tag{3.30}$$

Meanwhile, a comparison between $U_N^{n+1/2}$ and $U_N(\cdot\,, t^{n+1/2})$ shows that

$$U_N^{n+1/2} - U_N(\,\cdot\,, t^{n+1/2}) = \frac{1}{8}\Delta t^2 D_{t/2}^2 U_N^{n+1/2}. \tag{3.31}$$

Meanwhile, an application of Proposition 3.2 gives

$$\|D_{t/2}^2 \partial_x^4 U_N\|_{\ell^2(0,T)} \le C\|\partial_x^4 U_N\|_{H^2(0,T)}, \tag{3.32}$$

at each fixed grid point. As a result, we get

$$\|F_2 - \mathcal{I}(F_{2e})\|_{\ell^2(0,T;\ell^2)} \le C\Delta t^2 \|u_e\|_{H^2(0,T;H^4)}. \tag{3.33}$$

The terms F_3 and F_{3e} can be analyzed in the same way. We have

$$\|F_3 - \mathcal{I}(F_{3e})\|_{\ell^2(0,T;\ell^2)} \le C\Delta t^2 \|u_e\|_{H^2(0,T;H^2)}. \tag{3.34}$$

For the nonlinear terms F_4 and F_{4e}, we begin with the following estimate

$$\begin{aligned} \left\| F_4^{n+1/2} - \mathcal{I}\left(\partial_x^2 \left(\frac{3}{2}(U_N^p)^n - \frac{1}{2}(U_N^p)^{n-1}\right)\right)\right\|_2 &\le Ch^m \left\|\frac{3}{2}(U_N^p)^n - \frac{1}{2}(U_N^p)^{n-1}\right\|_{H^{m+2}} \\ &\le Ch^m \left(\|U_N^n\|_{H^{m+2}}^p + \|U_N^{n-1}\|_{H^{m+2}}^p\right) \le Ch^m \|U_N\|_{L^\infty(0,T;H^{m+2})}^p, \end{aligned} \tag{3.35}$$

with the first step based on the fact that $\frac{3}{2}(U_N^p)^n - \frac{1}{2}(U_N^p)^{n-1} \in \mathcal{B}^{pN}$. Meanwhile, the following observation

$$\frac{3}{2}(U_N^p)^n - \frac{1}{2}(U_N^p)^{n-1} - U_N^p(\cdot, t^{n+1/2}) = \frac{1}{8}\Delta t^2 D_{t/2}^2(U_N^p) - \frac{1}{2}\Delta t^2 D_t^2(U_N^p) \tag{3.36}$$

indicates that

$$\begin{aligned} &\left\| \mathcal{I}\left(\partial_x^2\left(\frac{3}{2}(U_N^p)^n - \frac{1}{2}(U_N^p)^{n-1}\right) - F_{4e}^{n+1/2}\right)\right\|_2 \\ &= \left\| \mathcal{I}\left(\partial_x^2\left(\frac{1}{8}\Delta t^2 D_{t/2}^2(U_N^p) - \frac{1}{2}\Delta t^2 D_t^2(U_N^p)\right)\right)\right\|_2 \\ &\le \frac{1}{8}\Delta t^2 \|D_{t/2}^2(U_N^p)\|_{H^{2+\eta}} + \frac{1}{2}\Delta t^2 \|D_t^2(U_N^p)\|_{H^{2+\eta}}, \quad \eta > \frac{1}{2}, \end{aligned} \tag{3.37}$$

with the last step coming from (2.4). Conversely, applications of Propositions 3.1 and 3.2 imply that

$$\|D_{t/2}^2(U_N^p)\|_{\ell^2(0,T;H^3)} \le C\|U_N^p\|_{H^2(0,T;H^3)}, \quad \|D_t^2(U_N^p)\|_{\ell^2(0,T;H^3)} \le C\|U_N^p\|_{H^2(0,T;H^3)}. \tag{3.38}$$

Note that an H^2 estimate (in time) is involved with a nonlinear term U_N^p. A detailed expansion in its first- and second-order time derivatives shows that

$$\partial_t(U_N^p) = pU_N^{p-1}\partial_t U_N, \quad \partial_t^2(U_N^p) = p(U_N^{p-1}\partial_t^2 U_N + (p-1)U_N^{p-2}(\partial_t U_N)^2), \tag{3.39}$$

which in turn leads to

$$\begin{aligned} \|U_N^p\|_{H^2(0,T)} &\le C(\|U_N\|_{L^\infty(0,T)}^{p-1} \cdot \|U_N\|_{H^2(0,T)} + \|U_N\|_{L^\infty(0,T)}^{p-2} \cdot \|U_N\|_{W^{1,4}(0,T)}^2) \\ &\le C\|U_N\|_{H^2(0,T)}^p, \end{aligned} \tag{3.40}$$

at each fixed grid point, with an 1D Sobolev embedding applied at the last step. Going back to (3.38) gives

$$\|D_{t/2}^2(U_N^p)\|_{\ell^2(0,T;H^3)} \le C\|U_N\|_{H^2(0,T;H^3)}^p, \quad \|D_t^2(U_N^p)\|_{\ell^2(0,T;H^3)} \le C\|U_N\|_{H^2(0,T;H^3)}^p. \tag{3.41}$$

A combination of (3.37), (3.41), and (3.35) leads to the consistency estimate of the nonlinear term

$$\|F_4 - \mathcal{I}(F_{4e})\|_{\ell^2(0,T;\ell^2)} \le C(\Delta t^2 + h^m)(\|u_e\|_{H^2(0,T;H^3)}^p + \|u_e\|_{L^\infty(0,T;H^{m+2})}^p). \tag{3.42}$$

Therefore, the local truncation error estimate for τ_1 is obtained by combining (3.29), (3.33), (3.34), and (3.42), combined with the consistency estimate (3.16) for U_N. Obviously, constant M only dependent on the exact solution u_e.

The estimate for τ_2 is very similar. We denote the following quantity

$$F_{5e}^{n+1/2} = \left(\partial_t U_N + \frac{\Delta t^2}{24}\partial_t^3 U_N\right)(\cdot, t^{n+1/2}). \tag{3.43}$$

A detailed Taylor formula in time gives the following estimate:

$$F_0^{n+1/2} - \mathcal{I}(F_{5e}^{n+1/2}) = \tau_{21}^{n+1/2}, \quad \text{with}$$
$$\|\tau_{21}\|_{\ell^2(0,T)} \le C\Delta t^3 \|U_N\|_{H^4(0,T)} \le C\Delta t^3 \|u_e\|_{H^4(0,T)}, \tag{3.44}$$

at each fixed grid point. Meanwhile, from the definition of (3.17), it is clear that F_5 has the following decomposition:

$$F_5^{n+1/2} = \frac{\Psi_N^{n+1}+\Psi_N^n}{2} = \frac{\partial_t U_N^{n+1}+\partial_t U_N^n}{2} - \frac{\Delta t^2}{12} \cdot \frac{\partial_t^3 U_N^{n+1}+\partial_t^3 U_N^n}{2} := F_{51}^{n+1/2} + F_{52}^{n+1/2}, \tag{3.45}$$

at a point-wise level. To facilitate the analysis below, we define two more quantities:

$$F_{51e}^{n+1/2} = \left(\partial_t U_N + \frac{\Delta t^2}{8}\partial_t^3 U_N\right)(\,\cdot\,, t^{n+1/2}), \quad F_{52e}^{n+1/2} = -\frac{\Delta t^2}{12}\partial_t^3 U_N(\,\cdot\,, t^{n+1/2}).$$

A detailed Taylor formula in time gives the following estimate:

$$F_{51}^{n+1/2} - \mathcal{I}(F_{51e}^{n+1/2}) = \tau_{22}^{n+1/2}, \quad F_{52}^{n+1/2} - \mathcal{I}(F_{52e}^{n+1/2}) = \tau_{23}^{n+1/2}, \quad \text{with}$$
$$\|\tau_{22}\|_{\ell^2(0,T)} \le C\Delta t^3 \|U_N\|_{H^4(0,T)} \le C\Delta t^3 \|u_e\|_{H^4(0,T)}, \tag{3.46}$$
$$\|\tau_{23}\|_{\ell^2(0,T)} \le C\Delta t^3 \|U_N\|_{H^4(0,T)} \le C\Delta t^3 \|u_e\|_{H^4(0,T)}, \tag{3.47}$$

at each fixed grid point. Consequently, a combination of (3.44)–(3.47) shows that

$$F_0^{n+1/2} - F_5^{n+1/2} = \tau_2^{n+1/2}, \quad \text{with } \|\tau_2\|_{\ell^2(0,T)} \le C\Delta t^3 \|u_e\|_{H^4(0,T)}. \tag{3.48}$$

This in turn implies that

$$\|F_0 - F_5\|_{\ell^2(0,T;\ell^2)} \le C\Delta t^3 \|u_e\|_{H^4(0,T;L^2)}. \tag{3.49}$$

Consequently, a discrete summation in Ω gives the second estimate in (3.23) (for $i = 2$), in which the constant M only dependent on the exact solution. The consistency analysis is thus completed. ■

IV. THE STABILITY AND CONVERGENCE ANALYSIS

Note that the numerical solution (u,ψ) of (2.10) is a vector function evaluated at discrete grid points. Before the convergence statement of the numerical scheme, its continuous extension in space is introduced, defined by $u_{\Delta t,h}^k = u_N^k$, $\psi_{\Delta t,h}^k = \psi_N^k$, in which $u_N^k, \psi_N^k \in \mathcal{B}^N, \forall k$, are the continuous version of the discrete grid functions u^k, ψ^k, with the interpolation formula given by (2.5).

The point-wise numerical error grid function is given by

$$\tilde{u}_i^n = U_i^n - u_i^n, \quad \tilde{\psi}_i^n = \Psi_i^n - \psi_i^n, \tag{4.1}$$

To facilitate the presentation below, we denote $(\tilde{u}_N^n, \tilde{\psi}_N^n) \in \mathcal{B}^N$ as the continuous version of the numerical solution $\tilde{u}^n$ and $\tilde{\psi}^n$, respectively, with the interpolation formula given by (2.5).

The following preliminary estimate will be used in later analysis. For simplicity, we assume the initial value for u_t for the GB equation (1.1) is given by $v^0(x) = u_t(x, t = 0) \equiv 0$. The general case can be analyzed in the same manner, with more details involved.

Lemma 4.1. *At any time step t^k, $k \geq 0$, we have*

$$||\tilde{u}_N^k||_{H^2} \leq C(||D_N^2 \tilde{u}^k||_2 + h^m), \tag{4.2}$$

Proof. First, we recall that the exact solution to the GB equation (1.1) is mass conservative, provided that $v^0(x) = u_t(x, t = 0) \equiv 0$:

$$\int_\Omega u_e(\cdot, t)\, dx \equiv \int_\Omega u_e(\cdot, 0)\, dx, \quad \text{with} \quad \forall t > 0. \tag{4.3}$$

Since U_N is the projection of u_e into $\mathcal{B}^N$, as given by (3.1), we conclude that

$$\int_\Omega U_N(\cdot, t)\, dx = \int_\Omega u_e(\cdot, t)\, dx \equiv \int_\Omega u_e(\cdot, 0)\, dx = \int_\Omega U_N(\cdot, 0)\, dx, \quad \text{with} \quad \forall t > 0. \tag{4.4}$$

Conversely, the numerical scheme (2.10) is mass conservative at the discrete level, provided that $\psi^0 \equiv 0$:

$$\overline{u^k} := h \sum_{i=0}^{N-1} u_i^k \equiv \overline{u^0} = \bar{C}_0. \tag{4.5}$$

Meanwhile, for $U_N^k \in \mathcal{B}^N$, for any $k \geq 0$, we observe that

$$\overline{U^k} = \int_\Omega U_N(\cdot, t^k)\, dx \equiv \int_\Omega U_N(\cdot, 0) = \overline{U^0}. \tag{4.6}$$

As a result, we arrive at a $O(h^m)$ order average for the numerical error function at each time step:

$$\overline{\tilde{u}^k} = \overline{U^k - u^k} = \overline{U^k} - \overline{u^k} = \overline{U^0} - \overline{u^0} = O(h^m), \quad \forall k \geq 0, \tag{4.7}$$

which comes from the error associated with the projection. This is equivalent to

$$\int_\Omega \tilde{u}_N^k\, dx = \overline{\tilde{u}^k} = O(h^m), \quad \forall k \geq 0, \tag{4.8}$$

with the first step based on the fact that $\tilde{u}_N^k \in \mathcal{B}^N$. As an application of elliptic regularity, we arrive at

$$||\tilde{u}_N^k||_{H^2} \leq C\left(\|\partial_x^2 \tilde{u}_N^k\|_{L^2} + \int_\Omega \tilde{u}_N^k\, dx\right) \leq C(\|D_N^2 \tilde{u}^k\|_2 + h^m), \tag{4.9}$$

in which the fact that $\tilde{u}_N^k \in \mathcal{B}^N$ was used in the last step. This finishes the proof of Lemma 4.1. ∎

Meanwhile, for a semidiscrete function w (continuous in space and discrete in time), the following norms are defined:

$$\|w\|_{\ell^\infty(0,T^*;H^k)} = \max_{0 \leq k \leq K} \|w^k\|_{H^k}, \quad \text{for any integer } k \geq 0. \tag{4.10}$$

Finally, we provide the detailed proof of Theorem 2.2, the main result of this article.

Proof. Subtracting (2.10) from (3.22) yields

$$\frac{\tilde{\psi}^{n+1}-\tilde{\psi}^{n}}{\Delta t} = -\frac{1}{2}D_N^4(\tilde{u}^{n+1}+\tilde{u}^n)+\frac{1}{2}D_N^2(\tilde{u}^{n+1}+\tilde{u}^n)+\tau_1^n + D_N^2\left(\frac{3}{2}\tilde{u}^n\sum_{k=0}^{p-1}(U^n)^k(u^n)^{p-1-k}-\frac{1}{2}\tilde{u}^{n-1}\sum_{k=0}^{p-1}(U^{n-1})^k(u^{n-1})^{p-1-k}\right), \tag{4.11}$$

$$\frac{\tilde{u}^{n+1}-\tilde{u}^{n}}{\Delta t} = \frac{\tilde{\psi}^{n+1}+\tilde{\psi}^{n}}{2}+\Delta t\tau_2^n. \tag{4.12}$$

Also note a $W^{2,\infty}$ bound for the constructed approximate solution

$$\|U_N\|_{L^\infty(0,T^*;W^{2,\infty})}\le C^*, \quad \text{that is}, \ \|U_N^n\|_{L^\infty}\le C^*, \|(U_N)_x^n\|_{L^\infty}\le C^*, \|(U_N)_{xx}^n\|_{L^\infty}\le C^*, \tag{4.13}$$

for any $n\ge 0$, which comes from the regularity of the constructed solution.

An a priori H^2 assumption up to time step t^n: We assume a priori that the numerical error function (for u) has an H^2 bound at time steps t^n, t^{n-1},

$$\|\tilde{u}_N^k\|_{H^2}\le 1, \quad \text{with } \tilde{u}_N^k=\mathcal{I}_N\tilde{u}^k, \quad \text{for } k=n,n-1, \tag{4.14}$$

so that the H^2 and $W^{1,\infty}$ bound for the numerical solution (up to t^n) is available

$$\begin{aligned}\|u_N^k\|_{H^2}&=\|U_N^k-\tilde{u}_N^k\|_{H^2}\le\|U_N^k\|_{H^2}+\|\tilde{u}_N^k\|_{H^2}\le C^*+1:=\tilde{C}_0,\\ \|u_N^k\|_{W^{1,\infty}}&\le C\|u_N^k\|_{H^2}\le C\tilde{C}_0:=\tilde{C}_1,\end{aligned} \tag{4.15}$$

for $k=n,n-1$, with an 1D Sobolev embedding applied at the final step.

Taking a discrete inner product with (4.11) by the error difference function $(\tilde{u}^{n+1}-\tilde{u}^n)$ gives

$$\begin{aligned}\left\langle\frac{\tilde{\psi}^{n+1}-\tilde{\psi}^{n}}{\Delta t},\tilde{u}^{n+1}-\tilde{u}^n\right\rangle &= \left\langle-\frac{1}{2}D_N^4(\tilde{u}^{n+1}+\tilde{u}^n),\tilde{u}^{n+1}-\tilde{u}^n\right\rangle\\ &+\left\langle D_N^2\left(\frac{3}{2}\tilde{u}^n\sum_{k=0}^{p-1}(U^n)^k(u^n)^{p-1-k}\right.\right.\\ &\left.\left.-\frac{1}{2}\tilde{u}^{n-1}\sum_{k=0}^{p-1}(U^{n-1})^k(u^{n-1})^{p-1-k}\right),\tilde{u}^{n+1}-\tilde{u}^n\right\rangle\\ &+\left\langle\frac{1}{2}D_N^2(\tilde{u}^{n+1}+\tilde{u}^n),\tilde{u}^{n+1}-\tilde{u}^n\right\rangle+\langle\tau_1^n,\tilde{u}^{n+1}-\tilde{u}^n\rangle.\end{aligned} \tag{4.16}$$

The leading term of (4.16) can be analyzed with the help of (4.12):

$$\left\langle\frac{\tilde{u}^{n+1}-\tilde{u}^{n}}{\Delta t},\tilde{\psi}^{n+1}-\tilde{\psi}^n\right\rangle=\left\langle\frac{\tilde{\psi}^{n+1}+\tilde{\psi}^{n}}{2}+\Delta t\tau_2^n,\tilde{\psi}^{n+1}-\tilde{\psi}^n\right\rangle$$

$$= \frac{1}{2}(\|\tilde{\psi}^{n+1}\|_2^2 - \|\tilde{\psi}^n\|_2^2) + \Delta t \langle \tau_2^n, \tilde{\psi}^{n+1} - \tilde{\psi}^n \rangle$$
$$\geq \frac{1}{2}(\|\tilde{\psi}^{n+1}\|_2^2 - \|\tilde{\psi}^n\|_2^2) - \frac{1}{2}\Delta t \|\tau_2^n\|_2^2 - \Delta t(\|\tilde{\psi}^{n+1}\|_2^2 + \|\tilde{\psi}^n\|_2^2). \tag{4.17}$$

The first term on the right-hand side of (4.16) can be estimated as follows.

$$\left\langle -\frac{1}{2}D_N^4(\tilde{u}^{n+1} + \tilde{u}^n), \tilde{u}^{n+1} - \tilde{u}^n \right\rangle = -\frac{1}{2}\langle D_N^2(\tilde{u}^{n+1} + \tilde{u}^n), D_N^2(\tilde{u}^{n+1} - \tilde{u}^n)\rangle$$
$$= -\frac{1}{2}(\|D_N^2\tilde{u}^{n+1}\|_2^2 - \|D_N^2\tilde{u}^n\|_2^2). \tag{4.18}$$

A similar analysis can be applied to the third term on the right-hand side of (4.16)

$$\left\langle \frac{1}{2}D_N^2(\tilde{u}^{n+1} + \tilde{u}^n), \tilde{u}^{n+1} - \tilde{u}^n \right\rangle = -\frac{1}{2}\langle D_N(\tilde{u}^{n+1} + \tilde{u}^n), D_N(\tilde{u}^{n+1} - \tilde{u}^n)\rangle$$
$$= -\frac{1}{2}(\|D_N\tilde{u}^{n+1}\|_2^2 - \|D_N\tilde{u}^n\|_2^2). \tag{4.19}$$

The inner product associated with the truncation error can be handled in a straightforward way:

$$\langle \tau_1^n, \tilde{u}^{n+1} - \tilde{u}^n \rangle = \frac{1}{2}\Delta t \langle \tau_1^n, \tilde{\psi}^{n+1} + \tilde{\psi}^n \rangle + \Delta t^2 \langle \tau_1^n, \tau_2^n \rangle$$
$$\leq \frac{1}{2}(\|\tilde{\psi}^{n+1}\|_2^2 + \|\tilde{\psi}^n\|_2^2) + \frac{1}{2}\Delta t \|\tau_1^n\|_2^2 + \frac{1}{2}\Delta t^2 \|\tau_2^n\|_2^2, \tag{4.20}$$

with the error equation (4.12) applied in the first step.

For nonlinear inner product, we start from the following decomposition of the nonlinear term:

$$\mathcal{NLT} = \mathcal{NLT}^1 + \mathcal{NLT}^2, \quad \text{with } \mathcal{NLT}^1 = \frac{3}{2}\tilde{u}^n \sum_{k=0}^{p-1} (U^n)^k (u^n)^{p-1-k},$$
$$\mathcal{NLT}^2 = -\frac{1}{2}\tilde{u}^{n-1} \sum_{k=0}^{p-1} (U^{n-1})^k (u^{n-1})^{p-1-k}. \tag{4.21}$$

For $\mathcal{NLT}^1$, we observe that each term appearing in its expansion can be written as a discrete interpolation form:

$$\tilde{u}^n (U^n)^k (u^n)^{p-1-k} = \mathcal{I}(\tilde{u}_N^n (U_N^n)^k (u_N^n)^{p-1-k}), \quad 0 \leq k \leq p-1, \tag{4.22}$$

so that the following equality is valid:

$$\|D_N^2(\tilde{u}^n (U^n)^k (u^n)^{p-1-k})\|_2 = \|\partial_x^2(\mathcal{I}_N(\tilde{u}_N^n (U_N^n)^k (u_N^n)^{p-1-k}))\|_{L^2}. \tag{4.23}$$

Conversely, we see that $\tilde{u}_N^n (U_N^n)^k (u_N^n)^{p-1-k} \in \mathcal{B}^{pN}$ (for each $0 \leq k \leq p-1$), so that an application of Lemma 2.1 gives

$$\|\partial_x^2(\mathcal{I}_N(\tilde{u}_N^n (U_N^n)^k (u_N^n)^{p-1-k}))\|_{L^2} \leq \sqrt{p}\|\tilde{u}_N^n (U_N^n)^k (u_N^n)^{p-1-k}\|_{H^2}. \tag{4.24}$$

Meanwhile, a detailed expansion for $\partial_x^j(\tilde{u}_N^n(U_N^n)^k(u_N^n)^{p-1-k})$ (for $0 \le j \le 2$) implies that

$$\|\partial_x^j(\tilde{u}_N^n(U_N^n)^k(u_N^n)^{p-1-k})\|_{L^2} \le C(\|U_N^n\|_{H^2}^{p-1} + \|u_N^n\|_{H^2}^{p-1} + 1)\|\tilde{u}_N^n\|_{H^2}, \quad 0 \le j \le 2, \tag{4.25}$$

with repeated applications of 1D Sobolev embedding, Hölder inequality and Young inequality. Furthermore, a substitution of the bound (4.13) for the constructed solution U_N and the a priori assumption (4.14) into (4.24) leads to

$$\|\tilde{u}_N^n(U_N^n)^k(u_N^n)^{p-1-k}\|_{H^2} \le C((C^*)^{p-1} + (\tilde{C}_1)^{p-1} + 1)\|\tilde{u}_N^n\|_{H^2}. \tag{4.26}$$

In turn, a combination of (4.23), (4.24), and (4.26) implies that

$$\|D_N^2(\tilde{u}^n(U^n)^k(u^n)^{p-1-k})\|_2 \le C((C^*)^{p-1} + (\tilde{C}_1)^{p-1} + 1)\|\tilde{u}_N^n\|_{H^2}. \tag{4.27}$$

This bound is valid for any $0 \le k \le p-1$. As a result, going back to (4.21), we get

$$\|D_N^2(\mathcal{NLT}^1)\|_2 \le \tilde{C}_2\|\tilde{u}_N^n\|_{H^2}, \quad \text{with } \tilde{C}_2 = C((C^*)^{p-1} + (\tilde{C}_0)^{p-1} + 1). \tag{4.28}$$

A similar analysis can be performed to $\mathcal{NLT}^2$ so that we have

$$\|D_N^2(\mathcal{NLT}^2)\|_2 \le \tilde{C}_2\|\tilde{u}_N^{n-1}\|_{H^2}. \tag{4.29}$$

These two estimates in turn lead to

$$\|D_N^2(\mathcal{NLT})\|_2 = \|D_N^2(\mathcal{NLT}^1)\|_2 + \|D_N^2(\mathcal{NLT}^2)\|_2 \le \tilde{C}_2(\|\tilde{u}_N^n\|_{H^2} + \|\tilde{u}_N^{n-1}\|_{H^2}). \tag{4.30}$$

Consequently, the nonlinear inner product can be analyzed as

$$\begin{aligned}
\langle D_N^2(\mathcal{NLT}), \tilde{u}^{n+1} - \tilde{u}^n\rangle &\le \Delta t\|D_N^2(\mathcal{NLT})\|_2 \cdot \left\|\frac{\tilde{u}^{n+1} - \tilde{u}^n}{\Delta t}\right\|_2 \\
&\le \tilde{C}_2\Delta t(\|\tilde{u}_N^n\|_{H^2} + \|\tilde{u}_N^{n-1}\|_{H^2}) \cdot \left(\frac{1}{2}(\|\tilde{\psi}^{n+1}\|_2 + \|\tilde{\psi}^n\|_2 + \Delta t\|\tau_2^n\|_2)\right) \\
&\le C\tilde{C}_2\Delta t(\|\tilde{u}_N^n\|_{H^2}^2 + \|\tilde{u}_N^{n-1}\|_{H^2}^2 + \|\tilde{\psi}^{n+1}\|_2^2 + \|\tilde{\psi}^n\|_2^2) + C\Delta t^3\|\tau_2^n\|_2^2 \\
&\le C\tilde{C}_2\Delta t(\|D_N^2\tilde{u}^n\|_2^2 + \|D_N^2\tilde{u}^{n-1}\|_2^2 + \|\tilde{\psi}^{n+1}\|_2^2 + \|\tilde{\psi}^n\|_2^2) \\
&\quad + C\Delta t^3\|\tau_2^n\|_2^2 + C\Delta t h^{2m},
\end{aligned} \tag{4.31}$$

in which the preliminary estimate (4.2), given by Lemma 4.1, was applied in the last step.

Therefore, a substitution of (4.18), (4.19), (4.20), and (4.31) into (4.16) results in

$$\begin{aligned}
\tilde{E}^{n+1} - \tilde{E}^n &\le \tilde{C}_3\Delta t(\|D_N^2\tilde{u}^n\|_2^2 + \|D_N^2\tilde{u}^{n-1}\|_2^2 + \|\tilde{\psi}^{n+1}\|_2^2 + \|\tilde{\psi}^n\|_2^2) \\
&\quad + C\Delta t(\|\tau_1^n\|_2^2 + \|\tau_2^n\|_2^2) \\
&\le C\Delta t(\tilde{E}^n + \tilde{E}^{n+1}) + CM^2(\Delta t^2 + h^m)^2,
\end{aligned} \tag{4.32}$$

with $\tilde{C}_3 = C\tilde{C}_2$, with an introduction of a modified energy for the error function

$$\tilde{E}^n = \frac{1}{2}(\|\tilde{\psi}^n\|_2^2 + \|D_N^2\tilde{u}^n\|_2^2 + \|D_N\tilde{u}^n\|_2^2).$$

As a result, an application of discrete Grownwall inequality gives

$$\tilde{E}^l \le \tilde{C}_4(\Delta t^2 + h^m)^2, \quad \forall 0 \le l \le K, \tag{4.33}$$

which is equivalent to the following convergence result:

$$\|\tilde{\psi}^l\|_2 + \|\tilde{u}_N^l\|_{H^2} \le \tilde{C}_4(\Delta t^2 + h^m), \quad \forall 0 \le l \le K. \tag{4.34}$$

Recovery of the H^2 a priori bound (4.14): With the help of the $\ell^\infty(0,T;H^2)$ error estimate (4.34) for the variable u, we see that the a priori H^2 bound (4.14) is also valid for the numerical error function $\tilde{u}_N$ at time step t^{n+1}, provided that

$$\Delta t \le (\tilde{C}_4)^{-\frac{1}{2}}, \quad h \le (\tilde{C}_4)^{-\frac{1}{m}}, \quad \text{with } \tilde{C}_6 \text{ dependent on } T.$$

This completes the convergence analysis, $\ell^\infty(0,T^*;H^2)$ for u, and $\ell^\infty(0,T^*;\ell^2)$ for ψ.

Moreover, a combination of (4.34) and the classical projection (3.2) leads to (2.11). The proof of Theorem 2.2 is finished. ■

Remark 4.2. One well-known challenge in the nonlinear analysis of pseudospectral schemes comes from the aliasing errors. For the nonlinear error terms appearing in (4.21), it is clear that any classical approach would not be able to give a bound for its second-order derivative in a pseudospectral set-up. However, with the help of the aliasing error control estimate given by Lemma 2.1, we could obtain an estimate for its discrete H^2 norm; see the detailed derivations in (4.22)–(4.31).

This technique is the key point in the establishment of a high order convergence analysis, $\ell^\infty(0,T^*;H^2)$ for u, and $\ell^\infty(0,T^*;\ell^2)$ for ψ. Without such an aliasing error control estimate, only a $\ell^\infty(0,T^*;\ell^2)$ convergence for u, and $\ell^\infty(0,T^*;\ell^2)$ convergence can be obtained for ψ, at the theoretical level; see the detailed discussions in an earlier work [10].

Remark 4.3. For the temporal discretization, our proposed numerical method (2.10) is unconditionally stable and convergent, for the time step size Δt in terms of spatial grid size h. This unconditional stability is due to the fact that it is an application of the trapezoidal rule for a first-order system in time, which turns out to be A-stable, and all the eigenvalues of the linear part of the spatial GB operator lie on the purely imaginary axis, in terms of $\psi = \partial_t u$ (instead of u). The nonlinear term, which lags behind in time because of the explicit treatment, does not play a crucial role in this stability analysis.

Conversely, we should remark that, this intuitive argument is not sufficient to theoretically justify the unconditional stability. The reason is that, ψ and $\partial_t u$ are not equivalent at the same time step, due to the temporal discretization, so that the linearized stability analysis is not directly applicable, although it provides an intuitive and useful view-point. For the theoretical justification, the detailed proof in this section is referred.

Remark 4.4. A severe stability condition $\Delta t \le Ch^2$ reported in De Frutos' earlier work [10] comes more from the technical difficulty in the theoretical analysis than an essential constraint in practical computations. In fact, for the following linear scheme, which corresponds to the numerical method (2.13), with only the fourth-order diffusion involved in the spatial GB operator:

$$\frac{u^{n+1} - 2u^n + u^{n-1}}{\Delta t^2} = -\frac{1}{4} D_N^4 (u^{n+1} + 2u^n + u^{n-1}), \tag{4.35}$$

a careful estimate shows its unconditional stability, by taking inner product by $u^{n+1} - u^{n-1}$. Also, see the related analysis by Dupont [47].

However, due to certain technical difficulties, for its combination with the nonlinear term as appeared in (2.13), the stability and convergence could only be justified under a severe constraint $\Delta t = O(h^2)$.

Again, the authors believe that such a stability condition only corresponds to a theoretical difficulty, and it may not be needed in practical computations.

Remark 4.5. For the following linear scheme, which corresponds to the numerical method (2.13), with only the second-order diffusion involved in the spatial GB operator:

$$\frac{u^{n+1} - 2u^n + u^{n-1}}{\Delta t^2} = D_N^2 u^n, \tag{4.36}$$

a careful estimate indicates its stability under a standard CFL condition: $\Delta t \le Ch$.

As a result, we conclude that the second-order numerical scheme presented in [10] is conditionally stable, and the stability condition is the standard CFL one: $\Delta t \le Ch$, from the practical view-point. The severe stability constraint $\Delta t = O(h^2)$ (as reported in [10]) is more associated with the theoretical difficulties.

In fact, an analysis of a similar numerical scheme has been provided in [3], in which the explicit centering was applied to all the terms associated with the spatial GB operator, with a finite difference approximation taken in the space.

Remark 4.6. The authors have also observed that, for the following numerical scheme, which is a slight modification of the one reported in [10]:

$$\frac{u^{n+1} - 2u^n + u^{n-1}}{\Delta t^2} = -\frac{1}{2} D_N^4 (u^{n+1} + u^{n-1}) + \frac{1}{2} D_N^2 (u^{n+1} + u^{n-1}) + D_N^2((u^n)^2), \tag{4.37}$$

an unconditional stability and convergence could be derived in a careful manner. The details are left to interested readers.

V. NUMERICAL RESULTS

In this section, we perform a numerical accuracy check for the fully discrete pseudospectral scheme (2.10). Similar to [10], the exact solitary wave solution of the GB equation (with $p = 2$) is given by

$$u_e(x, t) = -A\mathrm{sech}^2\left(\frac{P}{2}(x - c_0 t)\right), \tag{5.1}$$

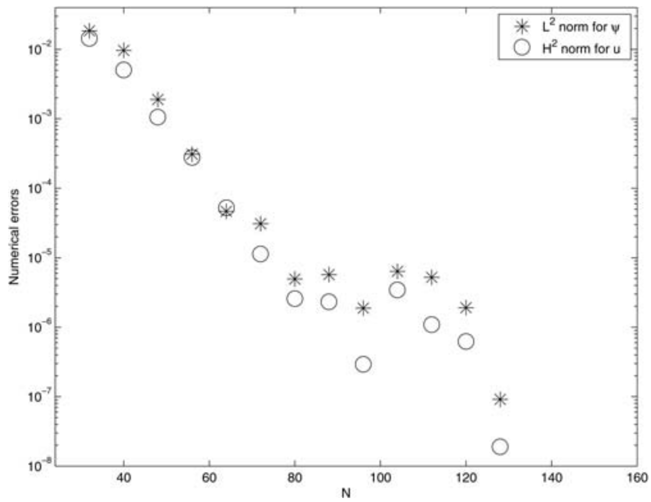

FIG. 1. Discrete L^2 numerical errors for $\psi = u_t$ and H^2 numerical errors for u at T = 4.0, plotted versus N, the number of spatial grid point, for the fully discrete pseudospectral scheme (2.10). The time step size is fixed as $\Delta t = 10^{-4}$. An apparent spatial spectral accuracy is observed for both variables.

in which $0 < P \leq 1$. In more detail, the amplitude A, the wave speed c_0 and the real parameter P satisfy

$$A = \frac{3P^2}{2}, \quad c_0 = (1 - P^2)^{1/2}. \tag{5.2}$$

Since the exact profile (5.1) decays exponentially as $|x| \to \infty$, it is natural to apply Fourier pseudospectral approximation on an interval $(-L,L)$, with L large enough. In this numerical experiment, we set the computational domain as $\Omega = (-40, 40)$. A moderate amplitude A = 0.5 is chosen in the test.

A. Spectral Convergence in Space

To investigate the accuracy in space, we fix $\Delta t = 10^{-4}$ so that the temporal numerical error is negligible. We compute solutions with grid sizes N = 32 to N = 128 in increments of 8, and we solve up to time T = 4. The following numerical errors at this final time

$$\|\psi - \psi_e\|_2, \quad \text{and} \quad \|D_N^2(u - u_e)\|_2, \tag{5.3}$$

are presented in Fig. 1. The spatial spectral accuracy is apparently observed for both u and $\psi = u_t$. Due to the fixed time step $\Delta t = 10^{-4}$, a saturation of spectral accuracy appears with an increasing N.

B. Second-Order Convergence in Time

To explore the temporal accuracy, we fix the spatial resolution as N = 512 so that the numerical error is dominated by the temporal ones. We compute solutions with a sequence of time step sizes, $\Delta t = \frac{T}{N_K}$, with N_K = 100 to N_K = 1000 in increments of 100, and T = 4. Figure 2 shows the

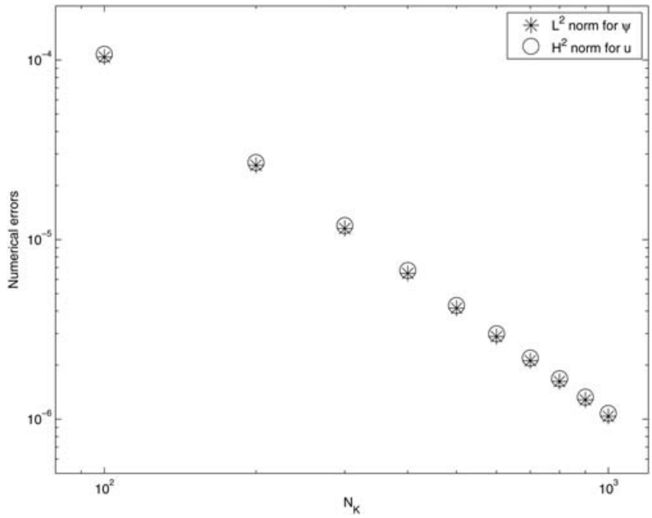

FIG. 2. Discrete L^2 numerical errors for $\psi = u_t$ and H^2 numerical errors for u at $T = 4.0$, plotted versus N_K, the number of time steps, for the fully discrete pseudospectral scheme (2.10). The spatial resolution is fixed as $N = 512$. The data lie roughly on curves CN_K^{-2}, for appropriate choices of C, confirming the full second-order temporal accuracy of the proposed scheme.

discrete L^2 and H^2 norms of the errors between the numerical and exact solutions, for $\psi = u_t$ and u, respectively. A clear second-order accuracy is observed for both variables.

VI. CONCLUDING REMARKS

In this article, we propose a fully discrete Fourier pseudospectral scheme for the GB equation (1.1) with second-order temporal accuracy. The nonlinear stability and convergence analysis are provided in detail. In particular, with the help of an aliasing error control estimate (given by Lemma 2.1, a $\ell^\infty(0, T^*; H^2)$ error estimate for u and $\ell^\infty(0, T^*; \ell^2)$ error estimate for $\psi = u_t$ are derived. Moreover, an introduction of an intermediate variable ψ greatly improves the numerical stability condition; an unconditional convergence (for the time step Δt in terms of the spatial grid size h) is established in this article, compared with a severe time step constraint $\Delta t \leq Ch^2$, reported in an earlier literature [10]. A simple numerical experiment also verifies this unconditional convergence, second-order accuracy in time, and spectral accuracy in space.

The authors greatly appreciate many helpful discussions with Panayotis Kevrekidis, in particular for his insightful suggestion and comments.

References

1. V. S. Manoranjan, A. R. Mitchell, and J. L. Morris, Numerical solutions of the good Boussinesq equation, SIAM Sci Stat Comput 5 (1984), 946–957.
2. V. S. Manotanjan, T. Ortega, and J. M. Sanz-Serna, Soliton and antisoliton interactions in the "good" Boussinesq equation, J Math Phys 29 (1988), 1964–1968.

3. T. Ortega and J. M. Sanz-Serna, Nonlinear stability and convergence of finite difference methods for the "good" Boussinesq equation, Numer Math 58 (1990), 215–229.

4. B. S. Attili, The Adomian decomposition method for solving the Boussinesq equation arising in water wave propagation, Numer Methods Partial Differential Equations 22 (2006), 1337–1347.

5. A. G. Bratsos, A predictor-corrector scheme for the improved Boussinesq equation, Chaos Solitons Fractals 40 (2009), 2083–2094.

6. A. G. Bratsos, A second order numerical scheme for the improved Boussinesq equation, Phys Lett A 370 (2007), 145–147.

7. R. Cienfuegos, E. Barthélemy, and P. Bonneton, A fourth-order compact finite volume scheme for fully nonlinear and weakly dispersive Boussinesq-type equations, Part I: Model development and analysis, Int J Numer Methods Fluids 51 (2006), 1217–1253.

8. R. Cienfuegos, E. Barthélemy, and P. Bonneton, A fourth-order compact finite volume scheme for fully nonlinear and weakly dispersive Boussinesq-type equations, Part II: Boundary conditions and validation, Int J Numer Methods Fluids 53 (2007), 1423–1455.

9. L. Farah and M. Scialom, On the periodic "good" Boussinesq equation, Proc Am Math Soc 138 (2010), 953–964.

10. J. De Frutos, T. Ortega, and J. M. Sanz-Serna, Pseudospectral method for the "good" Boussinesq equation, Math Comput 57 (1991), 109–122.

11. S. Gottlieb and C. Wang, Stability and convergence analysis of fully discrete Fourier collocation spectral method for 3-D viscous Burgers' equation, J Sci Comput 53 (2012), 102–128.

12. F. Linares and M. Scialom, Asymptotic behavior of solutions of a generalized Boussinesq type equation, Nonlinear Anal Theory Methods Appl 25 (1995), 1147–1158.

13. S. Oh and A. Stefanov, Improved local well-posedness for the periodic "good" Boussinesq equation, J Differ Equ 254 (2013), 4047–4065.

14. A. K. Pani and H. Saranga, Finite element Galerkin method for the "good" Boussinesq equation, Nonlinear Anal Theory Methods Appl 29 (1997), 937–956.

15. M. Tsutsumi and T. Matahashi, On the Cauchy problem for the Boussinesq type equation, Math Japonica 36 (1991), 371–379.

16. D. Gottlieb and S. A. Orszag, Numerical analysis of spectral methods, theory and applications, SIAM, Philadelphia, PA, 1977.

17. A. Majda, J. McDonough, and S. Osher, The Fourier method for non-smooth initial data, Math Comput 32 (1978), 1041–1081.

18. Y. Maday and A. Quarteroni, Legendre and Chebyshev spectral approximations of Burgers' equation, Numer Math 37 (1981), 321–332.

19. Y. Maday and A. Quarteroni, Approximation of Burgers' equation by pseudospectral methods, RAIRO Anal Numer 16 (1982), 375–404.

20. Y. Maday and A. Quarteroni, Spectral and pseudospectral approximation to Navier-Stokes equations, SIAM J Numer Anal 19 (1982), 761–780.

21. G. Q. Chen, Q. Du, and E. Tadmor, Super viscosity approximations to multi-dimensional scalar conservation laws, Math Comput 61 (1993), 629–643.

22. B.Y. Guo, H. P. Ma, and E. Tadmor, Spectral vanishing viscosity method for nonlinear conservation laws, SIAM J Numer Anal 39 (2001), 1254–1268.

23. Y. Maday, S. M. Ould Kaber, and E. Tadmor, Legendre pseudospectral viscosity method for nonlinear conservation laws, SIAM J Numer Anal 30 (1993), 321–342.

24. E. Tadmor, Convergence of spectral methods to nonlinear conservation laws, SIAM J Numer Anal 26 (1989), 30–44.

25. E. Tadmor, Shock capturing by the spectral viscosity method, Comput Methods Appl Mech Eng 80 (1990), 197–208.

26. E. Tadmor, Total variation and error estimates for spectral viscosity approximations, Math Comput 60 (1993), 245–256.

27. E. Tadmor, Burgers' equation with vanishing hyper-viscosity, Commun Math Sci 2 (2004), 317–324.

28. E. Weinan, Convergence of spectral methods for the Burgers' equation, SIAM J Numer Anal 29 (1992), 1520–1541.

29. E. Weinan, Convergence of Fourier methods for Navier-Stokes equations, SIAM J Numer Anal 30 (1993), 650–674.

30. B. Y. Guo, A spectral method for the vorticity equation on the surface, Math Comput 64 (1995), 1067–1069.

31. B. Y. Guo and W. Huang, Mixed Jacobi-spherical harmonic spectral method for Navier–Stokes equations, Appl Numer Math 57 (2007), 939–961.

32. B. Y. Guo, J. Li, and H. P. Ma, Fourier-Chebyshev spectral method for solving three-dimensional vorticity equation, Acta Math Appl Sin 11 (1995), 94–109.

33. Q. Du, B. Guo, and J. Shen, Fourier spectral approximation to a dissipative system modeling the flow of liquid crystals, SIAM J Numer Anal 39 (2001), 735–762.

34. B. Y. Guo and J. Shen, On spectral approximations using modified Legendre rational functions: application to the Korteweg-de Vries equation on the half line, Indiana Univ Math J 50 (2001), 181–204, (Special issue: Dedicated to Professors Ciprian Foias and Roger Temam).

35. A. Bressan and A. Quarteroni, An implicit/explicit spectral method for Burgers' equation, CALCOLO 23 (1986), 265–284.

36. Y. Maday and A. Quarteroni, Error analysis for spectral approximation of the Korteweg-de Vries equation, Math Model Numer Anal 22 (1988), 499–529.

37. B. Pelloni and V. A. Dougalis, Error estimates for a fully discrete spectral scheme for a class of nonlinear, nonlocal dispersive wave equations, Appl Numer Math 37 (2001), 95–107.

38. Z. Deng and H. Ma, Error estimate of the Fourier collocation method for the Benjamin-Ono equation, Numer Math Theory Methods Appl 2 (2009), 341–352.

39. Z. Deng and H. Ma, Optimal error estimates of the Fourier spectral method for a class of nonlocal, nonlinear dispersive wave equations, Appl Numer Math 59 (2009), 988–1010.

40. J. C. López-Marcos and J. M. Sanz-Serna, Stability and convergence in numerical analysis, III: Linear investigation of nonlinear stability, IMA J Numer Anal 7 (1988), 71–84.

41. J. Boyd, Chebyshev and Fourier spectral methods, 2nd Ed., Dover, New York, NY, 2001.

42. C. Canuto, M. Y. Hussani, A. Quarteroni, and T. A. Zang, Spectral methods: evolution to complex geometries and applications to fluid dynamics, Springer-Verlag, Berlin, 2007.

43. J. Hesthaven, S. Gottlieb, and D. Gottlieb, Spectral methods for time-dependent problems, Cambridge University Press, Cambridge, 2007.

44. C. Canuto and A. Quarteroni, Approximation results for orthogonal polynomials in Sobolev spaces, Math Comput 38 (1982), 67–86.

45. G. A. Baker, Error estimates for finite element methods for second order hyperbolic equations, SIAM J Numer Anal 13 (1976), 564–576.

46. A. Baskara, J. S. Lowengrub, C. Wang, and S. M. Wise, Convergence analysis of a second order convex splitting scheme for the modified phase field crystal equation, SIAM J Numer Anal 51 (2013), 2851–2873.

47. T. Dupont, Galerkin methods for first order hyperbolics: an example, SIAM J Numer Anal 10 (2009), 890–899.

48. H. El-Zoheiry, Numerical investigation for the solitary waves interaction of the “good” Boussinesq equation, Appl Numer Math 45 (2003), 161–173.

49. B. Y. Guo and J. Zou, Fourier spectral projection method and nonlinear convergence analysis for Navier-Stokes equations, J Math Anal Appl 282 (2003), 766–791.

50. Q. Lin, Y. H. Wu, R. Loxton, and S. Lai, Linear B-spline finite element method for the improved Boussinesq equation, J Comput Appl Math 224 (2009), 658–667.

51. F. L. Liu and D. L. Russell, Solutions of the Boussinesq equation on a periodic domain, J Math Anal Appl 192 (1995), 194–219.

52. A. Shokri and M. Dehghan, A not-a-knot meshless method using radial basis functions and predictor-corrector scheme to the numerical solution of improved Boussinesq equation, Comput Phys Commun 181 (2010), 1990–2000.

53. E. Tadmor, The exponential accuracy of Fourier and Chebyshev differencing methods, SIAM J Numer Anal 23 (1986), 1–10.

54. C. Wang and S. Wise, An energy stable and convergent finite-difference scheme for the modified phase field crystal equation, SIAM J Numer Anal 49 (2011), 945–969.

55. A. M. Wazwaz, Constructions of soliton solutions and periodic solutions of the Boussinesq equation by the modified decomposition method, Chaos Solitons Fractals 12 (2001), 1549–1556.

56. R. Xue, The initial-boundary value problem for the “good” Boussinesq equation on the bounded domain, J Math Anal Appl 343 (2008), 975–995.